Title
Differential Gene Expression Reveals Mitochondrial Dysfunction in an Imprinting Center Deletion Mouse Model of Prader–Willi Syndrome

Journal
Clinical and Translational Science, 6(5)

ISSN
1752-8054

Authors
Yazdi, Puya G
Su, Hailing
Ghimbovschi, Svetlana
et al.

Publication Date
2013-10-01

DOI
10.1111/cts.12083

Differential Gene Expression Reveals Mitochondrial Dysfunction in an Imprinting Center Deletion Mouse Model of Prader–Willi Syndrome

Puya G. Yazdi, M.D.[1,†], Hailing Su, M.D.[1,†], Svetlana Ghimbovschi, MD, Ph.D.[2,†], Weiwei Fan, Ph.D.[3–5], Pinar E. Coskun, M.D.[3,4], Angèle Nalbandian, Ph.D.[1], Susan Knoblach, Ph.D.[2], James L. Resnick, M.D.[6], Eric Hoffman, Ph.D.[2], Douglas C. Wallace, Ph.D.[3,7], and Virginia E. Kimonis, M.D., M.R.C.P.[1]

Abstract

Prader–Willi syndrome (PWS) is a genetic disorder caused by deficiency of imprinted gene expression from the paternal chromosome 15q11–15q13 and clinically characterized by neonatal hypotonia, short stature, cognitive impairment, hypogonadism, hyperphagia, morbid obesity, and diabetes. Previous clinical studies suggest that a defect in energy metabolism may be involved in the pathogenesis of PWS. We focused our attention on the genes associated with energy metabolism and found that there were 95 and 66 mitochondrial genes differentially expressed in PWS muscle and brain, respectively. Assessment of enzyme activities of mitochondrial oxidative phosphorylation complexes in the brain, heart, liver, and muscle were assessed. We found the enzyme activities of the cardiac mitochondrial complexes II+III were up-regulated in the PWS imprinting center deletion mice compared to the wild-type littermates. These studies suggest that differential gene expression, especially of the mitochondrial genes may contribute to the pathophysiology of PWS. Clin Trans Sci 2013; Volume 6: 347–355

Keywords: Prader–Willi syndrome, differential gene expression, PWS-IC mouse model

Introduction

Prader–Willi syndrome (PWS) is a complex neurodevelopmental disorder resulting from deficiency of imprinted gene expression from paternal chromosome 15q11–15q13.[1,2] PWS is characterized by multiple clinical manifestations during development and adulthood. *In utero* features include reduced fetal movement and polyhydramnios and in infancy, feeding difficulties, hypogonadism, hypotonia, and failure to thrive. During childhood, delayed motor speech development, behavioral abnormalities that include hyperphagia, and sleep disorder predominates. During adolescence, obesity, short stature, and delayed puberty are observed, and in adulthood, infertility, hypogonadism, cognitive impairment, and morbid obesity are significant problems. Dysmorphic features include bitemporal narrowing, upslanting palpebral fissures, and small hands and feet.[3]

The chromosome 15q11-q13 region contains imprinted sequences that are differentially expressed depending on the parent of origin. Due to imprinting, the maternally inherited copies of these genes are virtually silent, with only the paternal copies of the genes being expressed. In 70% of individuals, PWS results from the absence of paternally expressed imprinted genes located on chromosome 15q11-q13, including *SNRPN*, *NECDIN*, *MAGEL2*, and *MKRN3* genes along with clusters of snoRNAs: *SNORD64*, *SNORD107*, *SNORD108*, two copies of *SNORD109*, 29 copies of *SNORD116* (HBII-85), and 48 copies of *SNORD115* (HBII-52).[4,5] Maternal uniparental disomy (UPD) in which there are two maternal and no paternal copies of this region accounts for 30% of PWS cases. Deletion of the same region on the maternal chromosome causes Angelman syndrome. An imprinting center (IC) in *cis* regulates the establishment of parental specific allelic differences in DNA methylation, chromatin structure, and expression of genes in the PWS critical region. Although the 15q11-q13 defect underlies the PWS phenotype, the genes within the region do not appear to be directly responsible for the complex phenotype. Rather, it seems likely that the PWS phenotype results from dysregulation of multiple interconnected neurological and metabolic pathways.[6] The PWS critical region extends over nearly half of 15q11-q13 and contains multiple paternally expressed genes. The protein-coding genes, small nuclear ribonucleoprotein N (SNRPN), and its bicistronic partner SNRPN upstream reading frame (SNURF) have been mapped to the PWS critical region.[7,8] Families with microdeletions causing PWS localize the PWS-IC to 4.3 kb overlapping with *SNRPN* exon 1.[9] *SNURF* and *SNRPN* are paternally expressed and encode two different proteins within a single transcript.[6] *SNRPN/SNURF-SNRPN* exon1 is embedded in a CpG island with complete methylation on the maternal allele and complete absence of methylation on the paternal allele. Recent findings have shown that deletion of the 29 copies of the C/D box snoRNA *SNORD116* (HBII-85) appears to be the primary cause of PWS.[10]

The PWS-IC mouse model is a powerful tool that can be efficiently used to better understand the biochemical and cellular mechanisms involved in human PWS. There are now considerable insights from various deletions and other mutations in essential regulatory elements, such as the IC and one or more paternally expressed structural genes in the PWS domain that these loci are important in generating the PWS phenotype. Maternal UPD/paternal deficiency produce neonatal lethality in 100% of mice.[11] Similarly, a large deletion associated with a transgenic insertion caused lethality in 100% of the mice with paternal inheritance.[12] A 35-kb deletion of the putative IC causes complete lethality and an imprinting defect when inherited from male chimeras. Deletion of this IC abolishes local paternally derived gene expression and

[1]Division of Genetics and Metabolism, Department of Pediatrics, University of California, Irvine, California, USA; [2]Children's National Medical Center, Research Center Genetic Medicine, Washington, DC, USA; [3]Center for Molecular and Mitochondrial Medicine and Genetics, University of California, Irvine, California, USA; [4]Department of Biological Chemistry, University of California, Irvine, California, USA; [5]Salk Institute of Biological Studies, La Jolla, California, USA; [6]Department of Molecular Genetics and Microbiology, University of Florida College of Medicine, Gainesville, Florida, USA; [7]Center for Mitochondrial and Epigenomic Medicine, Children's Hospital of Philadelphia and Department of Pathology and Laboratory medicine, University of Pennsylvania, Philadelphia, Pennsylvania, USA.

[†]These individuals contributed equally to this work.

Correspondence: Virginia E. Kimonis (vkimonis@uci.edu)

DOI: 10.1111/cts.12083

results in PWS.[13] Both the position of the IC and its role in the coordinate expression of genes is conserved between mouse and human, therefore indicating that the mouse is a suitable model system in which to investigate the molecular function and pathophysiological implication of imprinting defects. A complete imprinting defect (UPD and the 35-kb deletion of the mouse IC) causes complete or severe lethality, whereas a partial imprinting defect (the 4.8-kb deletion of the Snrpn promoter) causes partial or lesser lethality.[14] Lack of *Pwcr1/MBII-85* snoRNA is critical for neonatal lethality in PWS mouse model.[15] Another deletion introduced into the germline using homologous recombination removed the coding exons for both *Snurf* and *SmN* and for *Ube3a* and removed all of the intervening 0.5–0.7 Mb of genomic DNA. This deletion from *Snrpn* to *Ube3a* on the paternal chromosome is associated with severe growth retardation, hypotonia, and approximately 80% lethality and position effects on expression of imprinted genes. The surviving mice with the *Snrpn-Ube3a* deletion were fertile and were not obese.[16] In all cases of lethality in the PWS mouse models, the abnormal phenotype occurs only with paternal deficiency and is associated with decreased movement and poor feeding immediately after birth.

Previous work involving whole genome microarrays using RNA isolated from lymphoblastoid cells from PWS patients has revealed significant differences in expression patterns of numerous genes related to normal neurodevelopment and function including serotonin receptor genes (e.g., *HTR2B*); genes involved in eating behavior and obesity (*ADIPOR2*, *MC2R*, *HCRT*, *OXTR*); *STAR* (a key regulator of steroid synthesis); and *SAG* (an arrestin family member which desensitizes G-protein-coupled receptors).[17] In addition, the same group also performed whole genome microarrays on a PWS-IC deletion (PWS-IC del) mouse model on RNA extracted from whole brain tissue within 24 hours after birth. Their results demonstrated two very significant differences: first, an increased expression of *Pomc* and *Mc5r*, the former of which is believed to be involved in eating behavior and the latter in thermoregulation; and second, decreased expression of three relatively uncharacterized transcripts that are expressed from the paternal allele under regulatory control of the IC (AK013560, BB3144814, BB182944).[17]

Mitochondria, in addition to playing perhaps the most prominent role of all organelles in energy metabolism, are central to many cellular functions including the generation of ATP, intracellular Ca2+ homeostasis, reactive oxygen species (ROS) biology, and apoptosis.[18] Mitochondria are one of the most abundant organelles in muscle and brain cells, responsible for producing the majority of energy through oxidative phosphorylation (OXPHOS). Many genes associated with neurodegenerative diseases are now known to regulate mitochondrial function.[19] Mitochondrial dysfunction has been implicated in Parkinson's disease,[20] Huntington's disease,[21] amyotrophic lateral sclerosis,[22] muscular dystrophy,[23] type 2 diabetes mellitus,[24] and collagen VI myopathies.[25]

Despite a lack of clinical or animal studies demonstrating efficacy, a high percentage of patients with PWS are being treated with co-enzyme Q10 (Co-Q10). A vitamin-like substance, Co-Q10 is present in most eukaryotic cells, primarily in the mitochondria where it is a component of the electron transport chain functioning as an electron acceptor from complexes I and II before passing on the electron to complex III. Unpublished data from our laboratory indicates that of the majority of patients on Co-Q10 derive some benefit mainly with regard to their energy level. To date, no double-blind study has been undertaken to study the effects of Co-Q10 on mitochondrial activity.

Given that previous findings have demonstrated differentially expressed genes involved in energy metabolism; that patients derive therapeutic benefit from supplementation with a mitochondrial component of the electron transport chain; the abundance of mitochondria in neuronal, liver, and skeletal muscle tissues; and that mitochondria play a central role in energy metabolism through ATP generation and pathophysiologic manifestations through ROS generation, we hypothesized that mitochondrial dysfunction is a pivotal component of PWS pathology.

We investigated the gene expression profiles of the quadriceps muscle and brain tissues in PWS-IC transgenic mouse model. Using RNA isolated from these tissues, we performed a comprehensive analysis of differential gene expression using the microarray approach with a goal to identify altered genes and link them to specific pathways that are relevant to PWS.

Methods

PWS-IC del mouse model

PWS-IC del mice were developed as described previously[26] and were kindly provided by Dr. Resnick (College of Medicine, University of Florida, Gainesville, FL, USA). All experiments were done with the approval of the Institutional Animal Care and Use Committee (IACUC Protocol #2007–2716–1) of the University of California, Irvine (UCI), and in accordance with the guidelines established by the NIH. All animals were housed in the vivarium of the UCI and maintained under constant temperature (22°C) and humidity with a controlled 12:12-hour light–dark cycle. PWS-IC del mice weighed approximately 16–20 g and wild-type (WT) littermates weighed approximately 30–35 g. All animals were 6 months old females and an F1 hybrid of WT friend leukemia virus B strain (FVB) females and B6 males bearing the 35-kb IC del mutation strains. Mutant mice were bred after culling all but one WT pup within a day of birth. So, the animals were presumed to have FVB mitochondria.

Electron microscopy

Mutant and WT mice tissues were fixed in 4% paraformaldehyde plus 0.1% glutaraldehyde in 0.1 M PB for 24 hours. Sections (100 μM) were cut with a vibratom, then collected in PBS and fixed in 1% glutaraldehyde overnight. Tissue samples were fixed in 1% osmium for 1 hour at 4°C and dehydrated in ethanol, which are embedded in eponate 12 resin at 65°C for 24–36 hours. Ultrathin (approximately 60–80 nm) sections were cut with a diamond knife and stained in 1% uranyl acetate for 30 minutes, followed by lead citrate for 7–10 minutes. Electron micrographs (EMs) were taken with a Gatan UltraScan US1000 digital camera and examined on a Philips CM10 transmission electron microscope.

Mitochondrial isolation and OXPHOS enzyme analysis

Mitochondria were isolated from the liver, heart, skeletal muscle (vastus lateralis), and the whole brain by homogenization and differential centrifugation as described previously.[27] Mitochondrial enzyme complex activities were determined by OXPHOS enzyme assays using our standard protocols.[6] In brief, equal amounts of mitochondrial proteins were assayed and normalized to citrate synthase (CS) activity, which remained at unchanged levels throughout the assay.

Complex I activity assay
A total of 80 µL of water, 100 µL of 2× buffer (500 mM sucrose, 2 mM EDTA, 100 mM Tris-HCl at pH 7.4), 2 µL of 10 mM decylubiquinone (Sigma-Aldrich, St. Louis, MO, USA), 0.5 µL of 2 M KCN, and 10 µL of 1 mg/mL mitochondria incubated for 5 minutes at 30°C. The reaction was started by adding 10 µL of 1 mM NADH, after which absorbance was measured at 340 nm for 5 minutes to quantify the rotenone-sensitive activity, which was determined in the presence of 1 µL of 1 mg/mL rotenone in a parallel experiment.

Complex II+III activity assay
The rate of cytochrome c (cytc) reduction was measured at 550 nm in a reaction containing 110 µL of water, 80 µL of 100 mM potassium phosphate buffer (pH 7.4), 4 µL of 1 M succinate, 1 µL of 0.1 M EDTA, 0.5 µL of 2M KCN, and 6 µL of 1 mM cytc. Note that, 5 µL of 1 mg/mL mitochondria was added and the absorption was monitored at 550 nm for 2 minutes.

Complex IV oxidation assay
The rate of cytc oxidation was measured at 550 nm in a reaction containing 170 µL of water, 20 µL of 100 mM potassium phosphate buffer (pH 7.4), and 10 µL of 1 mM reduced cytc. Note that, 5 µL of 0.1 mg/mL mitochondria was added. The absorption at 550 nm was monitored for 2 minutes. Reduced cytc was prepared by adding 2 µL of 1 M dithiothreitol to 1 mL of 1 mM cytc and incubated for 15 minutes.

CS activity assay
The reduction of 5,5′-dithio-bis (2-nitrobenzoic acid; DTNB) was measured at 412 nm in a reaction containing 160 µL of water, 20 µL of 1 M Tris-HCl (pH 8.0), 10 µL of 6 mM acetyl-CoA, and 2 µL of 10 mM DTNB by adding 5 µL of 1 mg/mL mitochondria. The absorption at 412 nm was monitored for 2 minutes.

Mitochondrial enzyme analysis
Measurements of mitochondrial enzyme activities were repeated three times for each test on each animal. The unpaired student's *t*-test was used to evaluate differences in WT and mutant values. Data represent mean ± SD. An analysis with a value of $p < 0.05$ was considered to be statistically significant.

Microarray analysis
Skeletal (quadriceps) and whole brain samples from the mutant mice ($n = 3$) and their WT age-matched littermates ($n = 4$) were analyzed by microarray technology using the Mouse Genome 430 2.0 arrays (Affymetrix, Santa Clara, CA, USA). Total RNA was extracted using a TRIzol-reagent (Invitrogen) and purified with RNeasy Mini kit (Qiagen , Valencia, CA, USA). RNA concentration was determined by spectrophotometry (Bio-Rad, Hercules, CA, USA) and the quality of RNA samples was assessed by Agilent 2100 Bioanalyzer (Agilent Technologies, Inc., Santa Clara, CA, USA). Note that, 2 µg of total high-quality RNA was used to start cDNA-cRNA synthesis by *in vitro* transcription using Affymetrix GeneChip® Expression 3′Amplification One-Cycle Target Labeling and Control Reagent kit. Double-stranded cDNA and Biotinylated cRNA were purified by Gene Chip Sample Cleanup Module (Affymetrix). Note that, 17 µg of biotinylated cRNAs from samples are fragmented, 15 µg of which were placed in a hybridization mixture of which 10 µg was hybridized to an Affymetrix Gene-Chips array for 16 hours. The arrays were washed and stained on the Affymetrix Fluidics Station 450 (Affymetrix) according to manufacturer's instructions. Briefly, nonspecifically bound material was removed and followed by incubation with phycoerythrin–streptavidin to detect bound cRNA. The signal intensity was amplified by second staining with biotin-labeled antistreptavidin antibody followed by phycoerythrin–streptavidin restaining. Fluorescent images were captured using the Affymetrix Gene Chip Scanner 3000 7G.

Gene expression profiling data analysis
Cell intensity file (CEL) image files were analyzed with the Probe Logarithmic Intensity Error algorithm (PLIER; Affymetrix). Unsupervised clustering of the data from all samples was performed with Hierarchical Clustering Explorer (HCE) 3. The PLIER data set was also analyzed with the data-mining program GeneSpring GX (version 7.3.1; Agilent Technologies, Inc.). Before screening for probe sets with altered expression levels, the data set, or signal intensities were normalized in two ways: (1) to each chip using a distribution of all genes around the 50th percentile; (2) to the mean values of infected sample's own control, so that all probe sets from control samples had a mean value of 1, and probe sets from mutant versus control samples had a value of either greater than, less than, or equal to 1, representing up-regulation, down-regulation, or no change, respectively. Only probe sets that were statistically significant via one-way ANOVA *t*-test with a *p*-value cutoff of $p < 0.001$ or $p < 0.01$ were considered further. Data were clustered as gene trees where yellow represents an expression ratio around 1, or no change (controls), and hotter colors (red = maximum) indicate an increase, and cooler colors (blue = minimum) indicate a decrease from control levels. For the generation of canonical pathways and networks, we used Ingenuity Pathways Analysis (IPA; Ingenuity Systems, Redwood City, CA, USA). The hyperlink of the GEO submission for study number GSE41759 is: http://www.ncbi.nlm.nih.gov/geo/query/acc.cgi?acc = GSE41759.

Quantitative real-time PCR (qRT-PCR)
Expression levels of genes that are most significantly differentially expressed (at least >1.5-fold difference) between control and mutant samples were confirmed by qRT-PCR using Roche LightCycler 480 Real-Time PCR System (Roche Applied Science, Indianapolis, IN, USA). Note that, 200 ng of total RNA were treated with DNAse I (Roche Diagnostics) before cDNA synthesis that was prepared using transcription kit and random hexamers (Applied Biosystems, Carlsbad, CA, USA). RT reactions were carried out in 20 µL according to manufacturer's protocol, and 1.8 µL of cDNA was used for each qRT-PCR reaction. In order to validate our microarray data, predesigned fluorogenic 6-carboxyfluorescein (FAM)-labeled primers/probes were used to measure transcription levels of the selected genes. Probes for the qRT-PCR validation were selected from Applied Biosystems Web site, and were used as sense/antisense primers. For the muscle tissue the following assays were used: Actc1 (ID: Mm00477277_g), Igfbpl1 (ID: Mm00497621_m1), Casr (ID: Mm00443375_m1), Mppe1 (ID: Mm00553989_m1), Tbc1d1 (ID: Mm00497989_m1); and for the brain tissue we used: Mrpl15 (ID: Mm00804108_m1) and Utrn (ID: Mm01168866_m1). Mouse GAPDH (Part Number 4352932E) was used as an endogenous control. All qRT-PCR results were normalized to control samples.

Results

Differentially expressed transcripts in the PWS-IC del mice and analysis of ingenuity networks

We analyzed gene expression from the skeletal muscle and brain tissues of the PWS-IC del mice by using whole genome microarray. Gene-clustering analysis of statistically significant ($p < 0.01$), differentially expressed genes revealed dysregulated expression of 726 genes in muscle and 332 genes in brain of PWS-IC mice as compared to littermate controls (*Figure 1*). We then grouped the genes that had a significant change in expression using IPA software (Ingenuity Systems) into bio-functional pathways for muscle and brain (*Figure 2* and *Table 1*). Statistically significant genes with the greatest fold change found in both muscle and brain are listed in *Table 2*. Of the differentially expressed genes, we found 95 and 66 mitochondrial genes differentially expressed in PWS-IC muscle and brain, respectively, at $p < 0.05$ (*Table 3*).

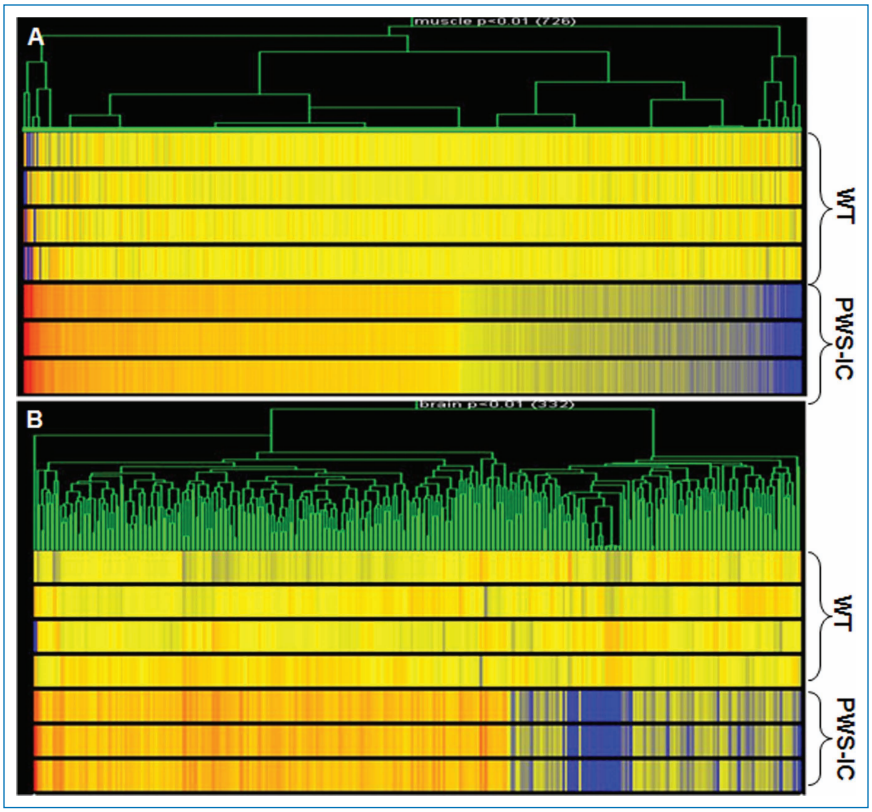

Figure 1. Genome microarray analysis of gene expression heat map in the skeletal muscle and brain samples of PWS-IC del mice. (A) Gene-based clustering for the genes in the skeletal muscle (726 genes) and (B) in the brain (332 genes) of the PWS-IC del mice from the Ingenuity's top network 1 ($p < 0.01$), analyzed together with 6 MD groups in Plier (normalization: per gene – to controls; per chip – to 50th percentile) compared to control littermates. Red color = up-regulated genes; blue color = down-regulated genes.

As predicted, all the known genes from the PWS critical region were down-regulated and *Ube3a* was significantly up-regulated. Previous microarray findings using a day old PWS mice[17] of which up-regulation of Mc5r (melanocortin receptor) and its interaction partner pro-opiomelanocortin (Pomc) were not observed. In order to validate our microarray data, we further investigated two significant genes in PWS muscle by RT-PCR. We confirmed that actin α cardiac muscle1 (Actc1) was up-regulated and Tre-2/Bub2/Cdc16 (TBC) domain family, member1 (Tbc1d1) was down-regulated in the PWS-IC del mice relative to their control littermates (*Figure 3*).

Analysis of mitochondrial complexes

To assess mitochondrial bioenergetic function, we assayed the relative activity of complexes I, II+III, and IV in skeletal muscle, liver, heart, and brain tissues of PWS-IC mice compared to their littermate controls. The data were normalized by CS activities.

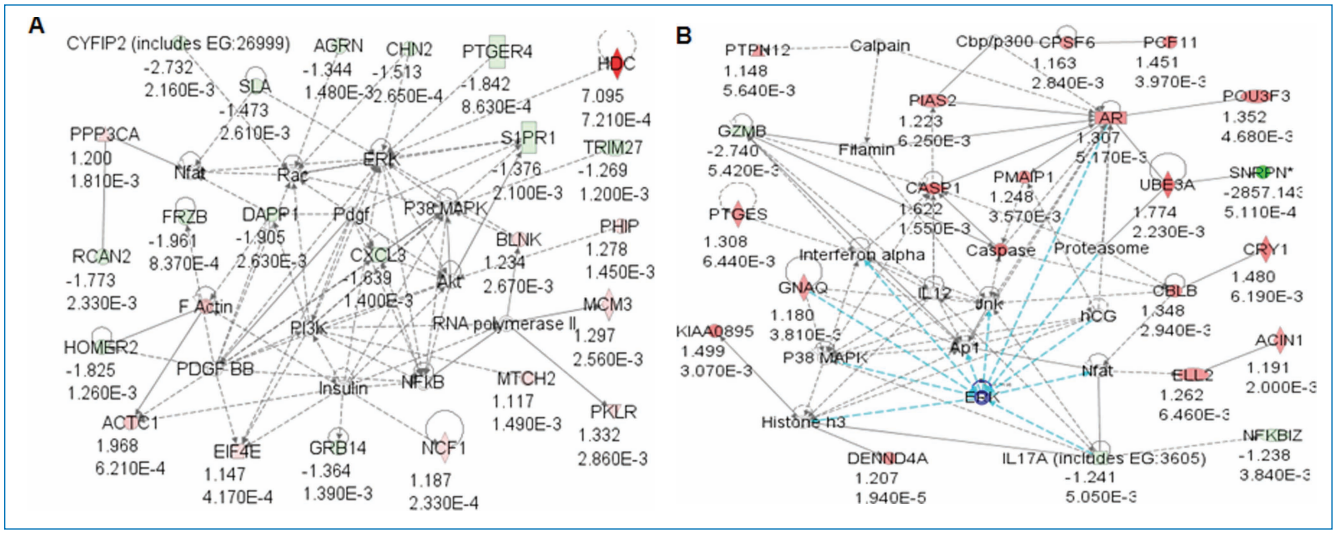

Figure 2. Network of bio-functional pathways in PWS-IC mouse skeletal muscle and brain. Genes with significant expression differences in (A) muscle tissue and (B) brain from PWS-IC del mice were grouped into Ingenuity networks by canonical pathways and signaling intermediates and bio-functional pathways using Ingenuity Pathways Analysis software.

Top biological functions (muscle)		
Diseases and disorders		
Name	p-Value	Number of genes
Cancer	8.02E-04–4.56E-02	29
Reproductive system disease	8.02E-04–4.56E-02	11
Developmental disorder	1.95E-03–1.64E-02	7
Genetic disorder	1.95E-03–4.95E-02	28
Inflammatory disease	3.10E-03–4.46E-02	9
Molecular cell functions		
Name	*p*-Value	Number of genes
Amino acid metabolism	3.66E-04–3.36E-02	6
Small molecule biochemistry	3.66E-04–4.19E-02	21
Cellular function and maintenance	1.95E-03–3.36E-02	3
Cellular movement	1.95E-03–4.19E-02	18
Carbohydrate metabolism	3.00E-03–3.36E-02	9
Physiological system development and function		
Name	*p*-Value	Number of genes
Skeletal and muscular system development and function	1.22E-03–3.36E-02	12
Tissue morphology	1.22E-03–3.36E-02	17
Nervous system development and function	1.47E-03–3.76E-02	12
Tissue development	1.47E-03–3.36E-02	9
Hematological system development and function	1.95E-03–4.19E-02	5
Top biological functions (brain)		
Diseases and disorders		
Name	*p*-Value	Number of genes
Developmental disorder	1.511E-03–2.95E-02	7
Genetic disorder	1.51E-03–3.68E-02	13
Neurological disease	5.46E-03–4.40E-02	15
Cancer	6.20E-03–4.63E-02	10
Reproductive system disease	6.20E-03–4.40E-02	8
Molecular cell functions		
Name	*p*-Value	Number of genes
Gene expression	1.5651E-04–4.40E-02	24
Cell morphology	3.29E-04–4.40E-02	8
Cellular development	3.29E-04–4.40E-02	8
Cellular growth and proliferation	3.29E-04–4.40E-02	9
Lipid metabolism	2.53E-03–5.00E-02	8
Physiological system development and function		
Name	*p*-Value	Number of genes
Cardiovascular system development and function	1.741E-04–4.40E-02	6
Organ development	1.74E-04–4.81E-02	14
Reproductive system development and function	3.29E-04–4.40E-02	4
Hematological system development and function	1.50E-04–4.40E-02	8
Immune cell trafficking	1.50E-03–5.00E-02	4

Table 1. List of biological functions as identified by Ingenuity in PWS-IC mouse muscle and brain samples ($p < 0.05$).

Up-regulated genes in PWS-IC muscle			
AFFY ID	**Gene symbol**	**Gene description**	**Fold change**
1452771_s_at	FACL3	Fatty acid coenzyme A ligase, long chain 3	1.44
1418911_s_at	FACL4	Fatty acid-coenzyme A ligase, long chain 4	1.38
1417434_at	GPD2	Glycerol phosphate dehydrogenase 2, mitochondrial	1.34
1429533_at	IMMT	Inner membrane protein, mitochondrial	1.32
1450612_a_at	PEMT	Phosphatidylethanolamine N-methyltransferase	1.31
1449137_at	PDHA1	Pyruvate dehydrogenase E1 alpha 1	1.268
1420044_at	NRD1	Nardilysin, N-arginine dibasic convertase, NRD convertase 1	1.26
1434996_at	SLC25A16	Solute carrier family 25 (mitochondrial carrier; Graves disease autoantigen), member 16	1.242
1453886_a_at	SLC25A26	Solute carrier family 25 (mitochondrial carrier; phosphate carrier), member 26	1.24
1429971_at	TXNRD2	Thioredoxin reductase 2	1.24
Down-regulated genes in PWS-IC muscle			
AFFY ID	Gene symbol	Gene description	Fold change
1452257_at	BDH	3-Hydroxybutyrate dehydrogenase (heart, mitochondrial)	−2.55
1422905_s_at	FMO2	Flavin containing monooxygenase 2	−2.04
1422997_s_at	MTE1	Mitochondrial acyl-CoA thioesterase 1	−1.66
1448988_at	ACADL	Acetyl-coenzyme A dehydrogenase, long-chain	−1.56
1430969_at	MTCH2	Mitochondrial carrier homolog 2 (C. elegans)	−1.55
1416203_at	AQP1	Aquaporin 1	−1.52
1450387_s_at	AK4	Adenylate kinase 4	−1.49
1422493_at	CPOX	Coproporphyrinogen oxidase	−1.47
1444394_at	ACAD9	Acyl-Coenzyme A dehydrogenase family, member 9	−1.42
1449443_at	DECR1	2,4-Dienoyl CoA reductase 1, mitochondrial	−1.39
1431148_at	AK3L	Adenylate kinase 3 alpha-like	−1.34
Up-regulated genes in PWS-IC brain			
AFFY ID	Gene symbol	Gene description	Fold change
1451623_at	MRPL15	Mitochondrial ribosomal protein L15	1.98
1458404_at	NDUFB8	NADH dehydrogenase (ubiquinone) 1 beta subcomplex 8	1.77
1417823_at	GCAT	Glycine C-acetyltransferase (2-amino-3-ketobutyrate-coenzyme A ligase)	1.55
1419362_at	MRPL35	Mitochondrial ribosomal protein L35	1.51
1421829_at	AK4	Adenylate kinase 4	1.46
1457790_at	ASB3	Ankyrin repeat and SOCS box-containing protein 3	1.45
1450948_a_at	MRPL1	Mitochondrial ribosomal protein L1	1.44
1421874_a_at	MRPS23	Mitochondrial ribosomal protein S23	1.41
1424164_at	MRPL50	Mitochondrial ribosomal protein L50	1.41
1422095_a_at	TYKI	Thymidylate kinase family LPS-inducible member	1.40
Down-regulated genes in PWS-IC brain			
AFFY ID	Gene symbol	Gene description	Fold change
1422008_a_at	AQP3	Aquaporin 3	−2100.84
1417614_at	CKM	Creatine kinase, muscle	−6.85
1431739_at	MTO1	Mitochondrial translation optimization 1 homolog (S. cerevisiae)	−1.95
1442331_at	ALAS1	Aminolevulinic acid synthase 1	−1.82
1430969_at	MTCH2	Mitochondrial carrier homolog 2 (C. Elegans)	−1.80
1444489_at	SLC25A12	Solute carrier family 25 (mitochondrial carrier, Aralar), member 12	−1.72
1441030_at	RAI14	Retinoic acid induced 14	−1.50
1453524_at	KIF5B	Kinesin family member 5B	−1.40
1418987_at	PLA2G2D	Phospholipase A2, group IID	−1.37
1440579_at	MIB1	Mindbomb homolog 1 (Drosophila)	−1.31

Table 2. Dysregulated mitochondrial genes in PWS-IC del mouse muscle and brain tissues (top 10-fold changes, $p < 0.05$).

GENES	Fold change
HDC	7.095
SYNTB1	4.346
ONECUT2	2.443
EGFL6	2.091
ZNF367	2.028
ACTC1	1.968
IGSF3	1.557
CILP	1.496
CASR	1.489
NUDT10	1.484
Down-regulated genes (muscle)	
GENES	Fold change
SNRPN	−537.63
NDN	−14.306
ANXA10	−13.158
GZMH	−13.021
NEU1	−2.770
CYFIP2	−2.732
TBC1D1	−2.252
DDAH1	−2.247
Up-regulated genes (brain)	
GENES	Fold change
MRPL15	1.975
ALOX18	1.859
CHRNA5	1.781
UBE3A	1.774
AMN	1.757
XBP1	1.684
DLEU2	1.675
CASP1	1.622
Down-regulated genes (brain)	
GENES	Fold change
SNRPN	−2857.1
NDN	−27.100
ANXA10	−2.793
SERPINA12	−2.747
GZMB	−2.740
VAX2	−2.160
C90RF165	−2.016
DDXR3Y	−2.008

Table 3. Top 10 list of dysregulated genes in PWS-IC del mouse muscle and brain tissues ($p < 0.05$) by Ingenuity.

The relative activities of mitochondrial complexes II+III were significantly up-regulated in cardiac muscle in PWS-IC del mice when compared to WT mice (student *t*-test, $p < 0.01$). Normalized complexes I, II+III, and IV activities in the brain, liver, and skeletal muscles were not significantly different between the PWS-IC del and WT mice (*Figure 4*).

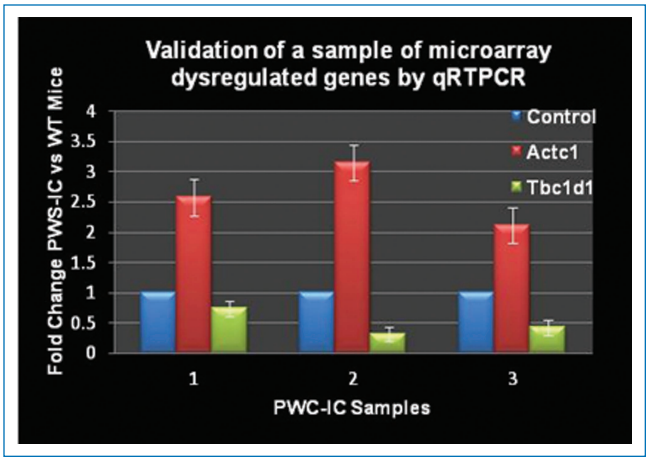

Figure 3. Validation of microarray genes in PWS-IC mouse model by qRT-PCR. Select genes were used for qRT-PCR analysis in order to validate the microarray data of PWS-IC and WT control littermates.

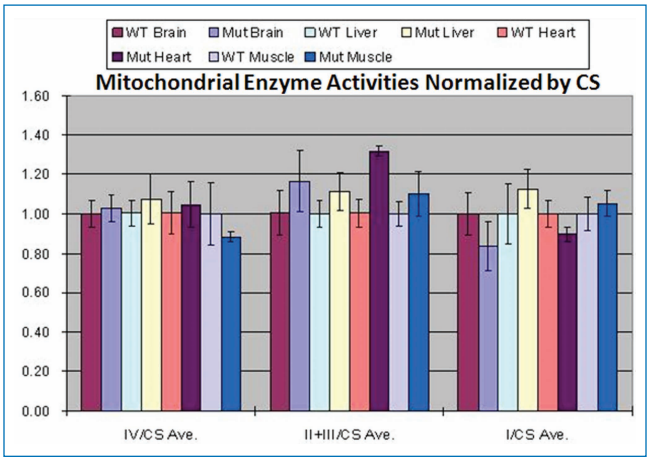

Figure 4. Complexes I, II+III, and IV activities in the brain, liver, heart, and skeletal muscles from PWS-IC and WT mice. The normalized complexes I and IV activities in the brain, liver, heart, and skeletal muscles and complexes II+III activities in the brain, liver, and skeletal muscles were not significantly different between the PWS-IC deletion and WT mice normalized to citrate synthase activity, which remained unchanged.

Mitochondrial EM structural changes

EM studies on cardiac and skeletal muscle tissues were reviewed in PWS-IC deletion mice compared to their WT littermate controls. We found abnormal mitochondrial proliferation, disorganized mitochondria swollen in appearance with disrupted membranes in both cardiac and skeletal muscle in PWS-IC del mouse as compared to littermate controls (*Figure 5*).

Discussion

PWS results from a loss of paternal imprinted genes from chromosome 15q11–15q13, leading to a profound disturbance of neurodevelopment that manifests multiple complex phenotypes including ones involved in energy metabolism, behavioral, cognitive, and structural defects. These complex clinical manifestations are the result of not only the loss of genes found on the deleted chromosome *per se*, but also the result of downstream changes in gene and regulatory networks involving those genes. Previous work has demonstrated that many of

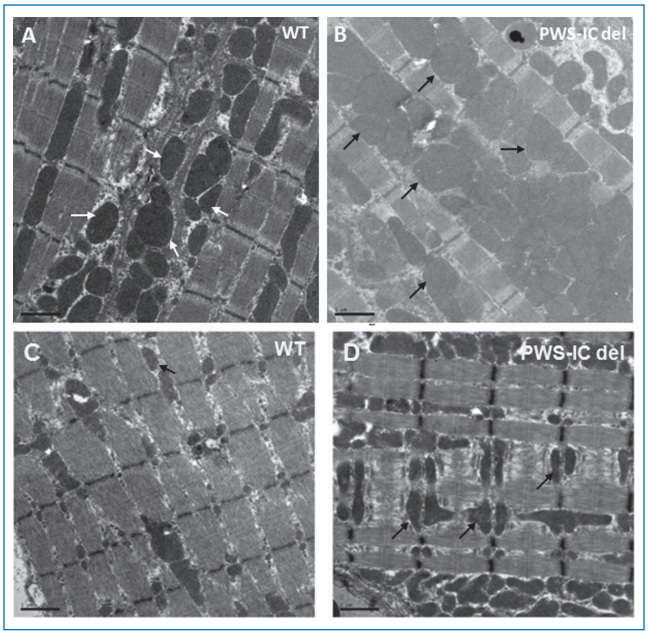

Figure 5. Electron microscopy of cardiac and skeletal muscle mitochondrial density in WT and PWS-IC del mice. (A) Cardiac and (C) muscle tissues from WT mice and (B) cardiac and (D) muscle tissues from PWS-IC del mice. Mutant samples demonstrate ultra structurally disorganized mitochondria, swollen in appearance with disrupted membranes (arrows) as compared to control littermates (Magnification 2950×).

the downstream-affected genes are involved in various energy metabolism pathways.[17] In addition, clinical evidence has shown a role for Co-Q10 supplementation in patient improvement. Thus far, to the best of our knowledge, no one had studied the possible role of mitochondrial dysfunction in PWS, we hypothesize that a component of PWS pathology is related to mitochondrial function.

We then conducted genome microarray analysis of RNA transcripts in skeletal muscle and brain tissues of our PWS-IC deletion mice, specifically looking for altered expression of genes involved in various mitochondrial pathways. We found 95 and 66 mitochondrial genes differentially expressed in WT and PWS-IC muscle and brain. As expected, all the known genes from the PWS critical region were down-regulated and *Ube3a* was significantly up-regulated.

Focusing our attention on transcripts that demonstrated a fold change (FC) of greater than 1.5 or less than −1.5, we discovered several mitochondrial genes that fall under cellular metabolism pathways by Ingenuity networks analysis. Specifically, in brain tissues *Mrpl15* (mitochondrial ribosomal protein L15) was up-regulated, while *Alas1* (aminolevulinic acid synthase 1) was down-regulated. *Mrpl15* encodes a 39s subunit protein that make up a part of the mitochondrial ribosome required for mitochondrial protein synthesis.[28] Recent bioinformatics approaches have linked this gene to possibly playing a role in stem cell pluripotency and differentiation.[29] *Alas1* gene product is a nuclear-encoded mitochondrial enzyme that is the rate-limiting and first enzyme in the heme biosynthetic pathway. A recent study has found down-regulated levels of this enzyme in Alzheimer's disease, possibly suggesting that down-regulated levels of this enzyme and dysfunctional heme metabolism could play a role in the cognitive and behavioral abnormalities seen in PWS.

In muscle tissues, we discovered the following down-regulated nuclear-coded mitochondrial gene expression levels; *Bdh* (3-hydroxybutyrate dehydrogenase) involved in fatty acid catabolism, *Mte1* (mitochondrial acyl-CoA thioesterase 1), involved in lipid metabolism pointing to a possible underlying mitochondrial role in biochemical metabolism pathways in PWS pathophysiology. *Acadl* (acetyl-Coenzyme A dehydrogenase, long-chain) belongs to the acyl-CoA dehydrogenase family of mitochondrial flavoenzymes involved in fatty acid and branched chain amino acid metabolism. The resulting protein is one of the four enzymes that catalyze the initial step of mitochondrial beta-oxidation of straight-chain fatty acid. Defects in this gene are the cause of long-chain acyl-CoA dehydrogenase deficiency, leading to nonketotic hypoglycemia [provided by RefSeq]. Finally, variants of *Mtch2* (mitochondrial carrier homolog 2) in humans have demonstrated a link with obesity[30] providing yet another potential clue to the role of mitochondrial dysfunction in the pathophysiology of PWS.

We have observed in a PWS-IC mouse model changes in muscle and brain mitochondrial gene expression and mitochondrial proliferation. We found significant structural changes on EM in cardiac cells of our PWS-IC del mouse model in addition to an increase of complex II+III activity in cardiac tissues.

These observations are consistent with previous reports of differential expression of energy metabolism genes and provide an explanation for possible therapeutic benefit from Co-Q10 supplementation. Co-Q10 plays a pivotal role as an electron acceptor from complex II before passing on those electrons to complex III. This study provides support for our hypothesis that PWS patients have an underlying defect in mitochondrial bioenergetics that is partially compensated by the up-regulation of mitochondrial biogenesis.

Conclusion

In conclusion, we have demonstrated ultra structural, enzymatic, and transcriptional changes of key mitochondrial components that point to a substantial role of mitochondrial dysfunction in the pathophysiology of PWS in the PWS-IC model. In addition, our microarray findings have detected previously unknown candidate genes that need to be studied in more detail to fully elucidate their potential role in PWS. In conclusion, this current work supports the rationale for Co-Q10 supplementation in PWS in alleviating some of the symptoms associated with this disease. Such studies could lead to other possible novel therapeutic avenues in treating this disease.

Acknowledgments

This research was supported by the Rare Diseases Clinical Research Consortia (USA), U54 RR019478, an RDCRN Post-doctoral trainee award and a Foundation of Prader-Willi Research (FPWR) grant (V.E.K.), California Regenerative Medicine Pre-doctoral Fellowship TI-00008 (W.F.), NICHD/NINDS 5R24HD050846-08: NCMRR-DC Core Molecular and Functional Outcome Measures in Rehabilitation Medicine, and the National Institute of Health (USA) grants NS21328, NS41850, AG13154, AG24373 and AG16573 (D.C.W.). We thank Fadia Haddad and Shlomit Aizik for helpful discussions.

References

1. Jiang Y, Tsai TF, Bressler J, Beaudet AL. Imprinting in Angelman and Prader–Willi syndromes. *Curr Opin Genet Dev.* 1998; 8(3): 334–342.

2. Nicholls RD, Knepper JL. Genome organization, function, and imprinting in Prader–Willi and Angelman syndromes. *Ann Rev Genom and Human Genet.* 2001; 2: 153–175.

3. Cassidy SB, Schwartz S, Miller JL, Driscoll DJ. Prader–Willi syndrome. *Genet Med.* 2011; 14(1): 10–26.

4. Cavaille J, Buiting K, Kiefmann M, Lalande M, Brannan CI, Horsthemke B, Bachellerie JP, Brosius J, Hüttenhofer A. Identification of brain-specific and imprinted small nucleolar RNA genes exhibiting an unusual genomic organization. *Proc Natl Acad Sci USA.* 2000; 97(26): 14311–14316.

5. delos Santos T, Schweizer J, Rees CA, Francke U. Small evolutionarily conserved RNA, resembling C/D box small nucleolar RNA, is transcribed from PWCR1, a novel imprinted gene in the Prader-Willi deletion region, which Is highly expressed in brain. *Am J Human Genet.* 2000; 67(5): 1067–1082.

6. Gray TA, Saitoh S, Nicholls RD. An imprinted, mammalian bicistronic transcript encodes two independent proteins. *Proc Natl Acad Sci USA.* 1999; 96(10): 5616–5621.

7. Nicholls RD, Saitoh S, Horsthemke B. Imprinting in Prader–Willi and Angelman syndromes. *Trends in Genet: TIG.* 1998; 14(5): 194–200.

8. Ning Y, Roschke A, Christian SL, Lesser J, Sutcliffe JS, Ledbetter DH. Identification of a novel paternally expressed transcript adjacent to snRPN in the Prader–Willi syndrome critical region. *Genome Res.* 1996; 6(8): 742–746.

9. Ohta T, Gray TA, Rogan PK, Buiting K, Gabriel JM, Saitoh S, Muralidhar B, Bilienska B, Krajewska-Walasek M, Driscoll DJ, Horsthemke B, Butler MG, Nicholls RD. Imprinting-mutation mechanisms in Prader–Willi syndrome. *Am J Human Genet.* 1999; 64(2): 397–413.

10. Sahoo T, del Gaudio D, German JR, Shinawi M, Peters SU, Person RE, Garnica A, Cheung SW, Beaudet AL. Prader–Willi phenotype caused by paternal deficiency for the HBII-85 C/D box small nucleolar RNA cluster. *Nature Genet.* 2008; 40(6): 719–721.

11. Cattanach BM, Barr JA, Evans EP, Burtenshaw M, Beechey CV, Leff SE, Brannan CI, Copeland NG, Jenkins NA, Jones J. A candidate mouse model for Prader–Willi syndrome which shows an absence of Snrpn expression. *Nature Genet.* 1992; 2(4): 270–274.

12. Gabriel JM, Merchant M, Ohta T, Ji Y, Caldwell RG, Ramsey MJ, Tucker JD, Longnecker R, Nicholls RD. A transgene insertion creating a heritable chromosome deletion mouse model of Prader–Willi and angelman syndromes. *Proc Natl Acad Sci USA.* 1999; 96(16): 9258–9263.

13. Yang T, Adamson TE, Resnick JL, Leff S, Wevrick R, Francke U, Jenkins NA, Copeland NG, Brannan CI. A mouse model for Prader–Willi syndrome imprinting-centre mutations. *Nature Genet.* 1998; 19(1): 25–31.

14. Bressler J, Tsai TF, Wu MY, Tsai SF, Ramirez MA, Armstrong D, Beaudet AL. The SNRPN promoter is not required for genomic imprinting of the Prader–Willi/Angelman domain in mice. *Nature Genet.* 2001; 28(3): 232–240.

15. Ding F, Prints Y, Dhar MS, , Johnson DK, Garnacho-Montero C, Nicholls RD, Francke U. Lack of Pwcr1/MBII-85 snoRNA is critical for neonatal lethality in Prader–Willi syndrome mouse models. *Mamm Genome.* 2005; 16(6): 424–431.

16. Tsai TF, Jiang YH, Bressler J, Armstrong D, Beaudet AL. Paternal deletion from Snrpn to Ube3a in the mouse causes hypotonia, growth retardation and partial lethality and provides evidence for a gene contributing to Prader–Willi syndrome. *Human Mol Genet.* 1999; 8(8): 1357–1364.

17. Bittel DC, Kibiryeva N, Talebizadeh Z, Butler MG. Microarray analysis of gene/transcript expression in Prader–Willi syndrome: deletion versus UPD. *J Med Genet.* 2003; 40(8): 568–574.

18. Wallace DC. A mitochondrial paradigm of metabolic and degenerative diseases, aging, and cancer: a dawn for evolutionary medicine. *Ann Rev Genet* 2005; 39: 359–407.

19. Keating DJ. Mitochondrial dysfunction, oxidative stress, regulation of exocytosis and their relevance to neurodegenerative diseases. *J Neurochem* 2008; 104(2): 298–305.

20. Betarbet R, Sherer TB, MacKenzie G, Garcia-Osuna M, Panov AV, Greenamyre JT. Chronic systemic pesticide exposure reproduces features of Parkinson's disease. *Nature Neurosci.* 2000; 3(12): 1301–1306.

21. Milakovic T, Johnson GV. Mitochondrial respiration and ATP production are significantly impaired in striatal cells expressing mutant huntingtin. *J Biol Chem.* 2005; 280(35): 30773–30782.

22. Mattiazzi M, D'Aurelio M, Gajewski CD, Martushova K, Kiaei M, Beal MF, Manfredi G. Mutated human SOD1 causes dysfunction of oxidative phosphorylation in mitochondria of transgenic mice. *J Biol Chem.* 2002; 277(33): 29626–29633.

23. Angelin A, Bonaldo P, Bernardi P. Altered threshold of the mitochondrial permeability transition pore in Ullrich congenital muscular dystrophy. *Biochim Biophys Acta.* 2008; 1777(7–8): 893–896.

24. Pagel-Langenickel I, Schwartz DR, Arena RA, Minerbi DC, Johnson DT, Waclawiw MA, Cannon RO 3rd, Balaban RS, Tripodi DJ, Sack MN. A discordance in rosiglitazone mediated insulin sensitization and skeletal muscle mitochondrial content/activity in Type 2 diabetes mellitus. *Am J Physiol Heart Circ Physiol.* 2007; 293(5): H2659–H2666.

25. Irwin WA, Bergamin N, Sabatelli P, Reggiani C, Megighian A, Merlini L, Braghetta P, Columbaro M, Volpin D, Bressan GM, Bernardi P, Bonaldo P. Mitochondrial dysfunction and apoptosis in myopathic mice with collagen VI deficiency. *Nature Genet.* 2003; 35(4): 367–371.

26. Chamberlain SJ, Johnstone KA, DuBose AJ, Simon TA, Bartolomei MS, Resnick JL, Brannan CI. Evidence for genetic modifiers of postnatal lethality in PWS-IC deletion mice. *Human Mol Genet.* 2004; 13(23): 2971–2977.

27. Trounce IA, Kim YL, Jun AS, Wallace DC. Assessment of mitochondrial oxidative phosphorylation in patient muscle biopsies, lymphoblasts, and transmitochondrial cell lines. *Methods in Enzymol.* 1996; 264: 484–509.

28. Kenmochi N, Suzuki T, Uechi T, Magoori M, Kuniba M, Higa S, Watanabe K, Tanaka T. The human mitochondrial ribosomal protein genes: mapping of 54 genes to the chromosomes and implications for human disorders. *Genomics* 2001; 77(1–2): 65–70.

29. Mason MJ, Fan G, Plath K, Zhou Q, Horvath S. Signed weighted gene co-expression network analysis of transcriptional regulation in murine embryonic stem cells. *BMC Genomics.* 2009; 10: 327.

30. Renstrom F, Payne F, Nordstrom A, Brito EC, Rolandsson O, Hallmans G, Barroso I, Nordström P, Franks PW; GIANT Consortium. Replication and extension of genome-wide association study results for obesity in 4923 adults from northern Sweden. *Human Mol Genet.* 2009; 18(8): 1489–1496.